Vacuum bag moulding of large thermoplastic parts in commingled glass/PET copolymer

A. G. Gibson, M. Ijaz, N. Dodds, A. Sharpe and H. Knudsen

This paper describes the development of a thermoplastic composite system for structural application in the chassis of an electrically propelled bus. The work involved the characterisation and modelling of a vacuum bag moulding process using a woven commingled thermoplastic composite precursor. The matrix materials were PET and a PET copolymer. The process employs an ambient pressure oven, with tooling that can be made from composite, metal or ceramic. The process results in good quality laminates, with a void content generally lower than 1%. The temperature profile through the part and the consolidation behaviour were characterised and modelled. It was found that the thermal profile could be modelled with adequate accuracy using 'single point' values of thermal properties. Experimental measurements showed, for the first time, that consolidation occurs in two stages: a low temperature solid state debulking near to T_g, followed by full melt impregnation at a higher temperature (above T_m in the case of the homopolymer). Both stages in the consolidation process were modelled separately using a simplified version of the Kamal equation. PRC/1818

 A. G. Gibson (a.g.gibson@ncl.ac.uk), M. Ijaz and N. Dodds are at the University of Newcastle upon Tyne, NE1 7RU, UK; A. Sharpe is with PERA Technology, Melton Mowbray, UK; and H. Knudsen is with Trevira Neckelmann, Denmark. This paper was presented at the 9th international conference on Fibre Reinforced Composites, FRC2002, held in Newcastle upon Tyne on 26–28 March 2002. Manuscript accepted in final form 6 March 2003.

INTRODUCTION

This project involved the development and characterisation of a vacuum bag process for the manufacture of thermoplastic composite parts on a size and scale suitable for lightweight public transport vehicles. The study centred on the replacement of load bearing chassis components of the electric bus shown in Fig. 1. One of the challenges of the project was the use of tooling made from a composite with a polymeric matrix. This posed some problems due to the high processing temperatures (in the range 200–300°C), which limited the range of tooling materials that could be used. Of course metal tooling may be employed for this application, and certain ceramic based materials[1] have also been found to be viable.

1 Electrically propelled bus – subject of case study (courtesy Robert Wright and Son, Belfast)

However, for medium volume production runs of larger parts, polymer composite tooling offers many attractions, including the ease with which doubly curved shapes can be produced. Moreover, improved resin chemistry has resulted in composite tooling with significantly improved high temperature capability. In the present project, glass–cyanate ester tools were supplied by ACG of Heanor, UK. These were found to work well with the PET copolymer for repeated mouldings.

The benefits of using thermoplastic composite technology[1–5] include emission free processing and recyclability of both intermediate factory scrap and final product. Since both the homopolymer and the copolymer used in the present study are derivatives of PET, the starting material can, in principle, be derived from the established PET recyclate stream. The availability of a lightweight thermoplastic composite will also promote the use of energy efficient transport.

Thermoplastic composites have been investigated for several transport applications, but attention to date has focused mainly on polypropylene (PP) matrixes.[2] This has occurred mainly because PP composites are the most generally available thermoplastic composite systems and also because many unreinforced thermoplastic mouldings employ PP for reasons of recyclability. However, PP is non-polar, and has a relatively low T_g of ~0°C. These factors taken together limit the interlaminar properties that can be achieved in PP composites. This can be a problem for structural applications, since both compressive strength and flexural strength are strongly related to intralaminar shear strength.

DOI 10.1179/146580103225002605

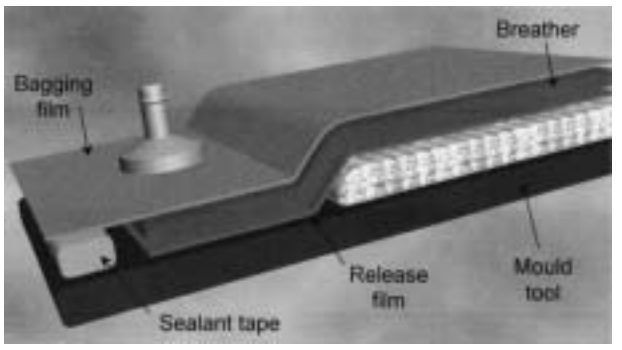

2 Schematic diagram showing bagging components prior to processing

Poly(ethylene terephthalate) based thermoplastic polyesters offer one solution to this problem.[1] Commingled precursor 'Comfil' was supplied by Trevira Neckelmann a.s. in the form of a woven twill fabric. The PET homopolymer gives tough laminates with a semicrystalline matrix,[1] but requires processing at 280°C. Because of the thermal limitations of lower cost bagging materials and other system components, a PET copolymer processable at 210–230°C was also employed. This was amorphous ($T_g = 60$°C) and somewhat similar mechanically to thermosetting polyester, albeit somewhat tougher.

The construction of a typical bagged part using the system described is shown in Fig. 2. One component investigated in the study was a large, highly loaded battery tray, with overall dimensions $\sim 1{\cdot}5 \times 3$ m. Figure 3 shows the composite tooling for this part, along with a bagged component ready for processing.

After optimising the process cycle to achieve good wetout, the extent of impregnation, as observed by optical microscopy and measured through void content, was found to be very good, void contents lower than 1% being typical. Properties of thermoplastic polyester–glass laminates compared very well with

3 Tooling for battery tray, made from composite with cyanate ester matrix (ACG), and bagged component prior to processing

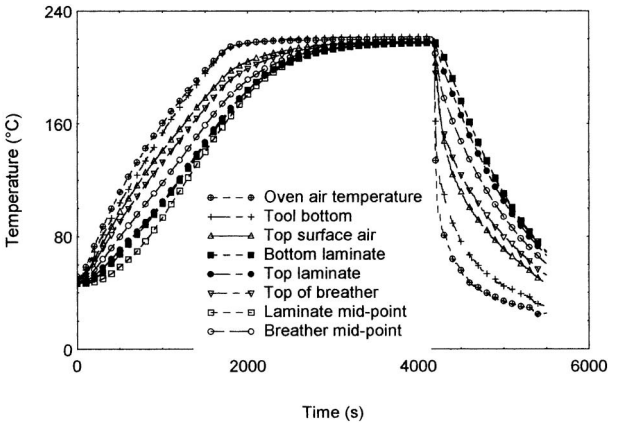

4 Thermocouple outputs during Comfil processing cycle for thermoplastic composite with copolyester matrix

their thermosetting counterparts, typical values being 15 GPa flexural modulus, 400 MPa flexural strength and 40 MPa interlaminar shear strength. The glass transition temperature was about 60°C. The manufacture of stiffened parts, using cores and sandwich construction was also investigated, along with methods of providing inserts and attachments.

PROCESS MODELLING AND DEVELOPMENT

Thermal modelling

Before producing tooling for large parts, trials were carried out with a 0·5 m square composite tool, supplied by ACG, Heanor UK. This was capable of operating at up to 300°C. Aluminium tooling was also investigated. The commingled precursor fabric was placed on the tool and covered with a breather fabric (Airbleed 33N) and flexible membrane, as shown in Fig. 2, prior to being evacuated and placed in an air circulating oven. Suitable proprietary membrane materials were identified and sourced, and process cycles with different temperature profiles were investigated. Figure 4 shows the temperatures recorded during a typical process cycle. This particular cycle employed 20 plies of commingled fabric which, after consolidation, gave a laminate thickness of 10 mm.

To model the thermal profile, a finite difference model was implemented, incorporating the key components membrane, breather, laminate and tooling. After some experimentation it was found that 50 spacial increments were sufficient to achieve accurate stable solutions. To establish thermal constants and external heat transfer coefficients, several instrumented heating and cooling experiments were carried out, to be reported in detail in a future publication. The thermal properties were derived by adjusting them to achieve the best fit with the observed response. Surprisingly it was found that most of the cycle could be fitted with reasonable accuracy using single 'average' values of the thermal constants over the temperature range. These are shown in Table 1.

Figure 5 shows a comparison of the measured and modelled thermal profile during consolidation, along with the modelling error. A simple reason why single point values work in the present case is apparent if one assumes the dominant thermal quantity to be the

prc0001818 01-04-03 16:38:26 Rev 14.05
The Charlesworth Group, Huddersfield 01484 517077

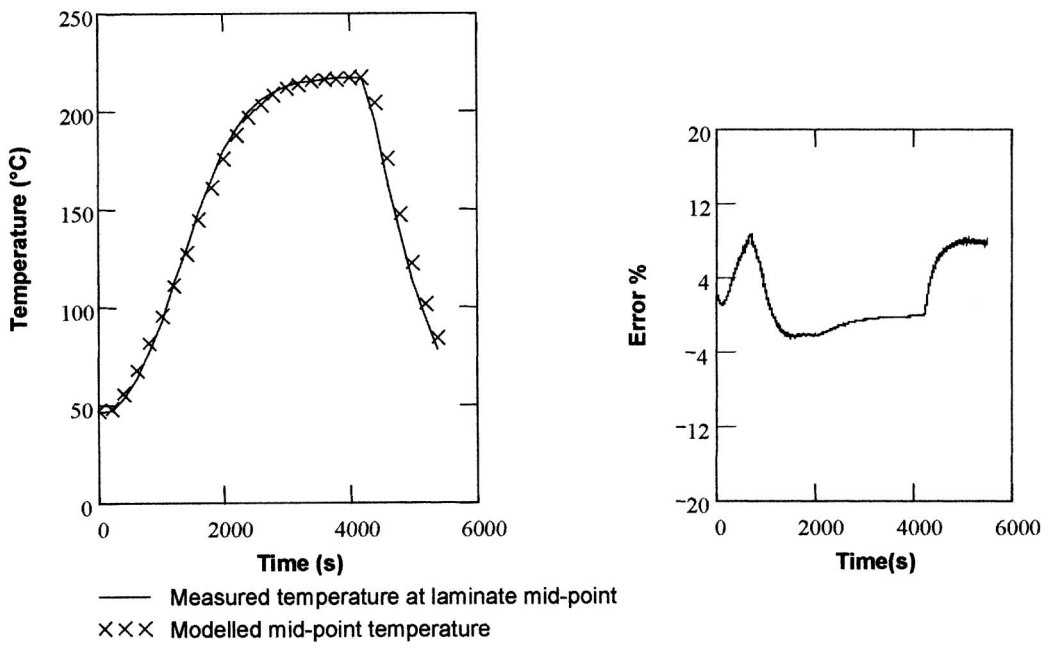

5 Comparison of measured laminate centreline temperature during process cycle (from Fig. 4) with values calculated from oven temperature profile, modelled using single point thermal values

thermal diffusivity α of the consolidating material. This, of course, is related to the thermal conductivity, density and specific heat by

$$\alpha = k/\rho C_p$$

Clearly, both the thermal conductivity and the bulk density of the commingled fabric increase considerably during the processing cycle. However, if they both vary in the same manner, and if the specific heat does not change much, then α will remain roughly constant.

It would be very surprising if the single point value assumption held for all classes of commingled composite, so work is continuing on materials characterisation to ascertain more accurately the evolution of the thermal properties of commingled fabrics during processing.

CONSOLIDATION MODELLING

Several workers have carried out experimental and modelling studies of the consolidation behaviour of commingled composites.[6–15] Probably the most widely used experimental technique for such studies has been constant velocity isothermal compaction, generally employing a mechanical testing machine or an instrumented press. This method had achieved some success in characterising the consolidation behaviour of both powder impregnated composites and commingled ones. To model the consolidation behaviour of the prepreg in the present case it was originally intended to use constant velocity consolidation experiments of the same type. However, isothermal consolidation

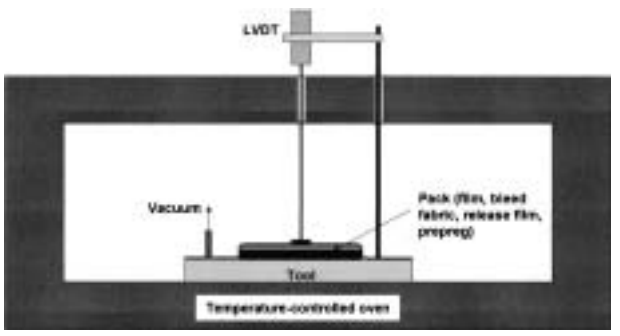

6 LDVT probe for measuring consolidation during processing

proved unsuitable because the effective pressures encountered in vacuum moulding, being just under 1 bar (1 bar = 10^5 Pa), are much lower than those normally imposed in consolidation testing.

With vacuum bag consolidation of commingled fabric the rate determining process is the heating and softening of the thermoplastic component, rather than the speed at which the laminate is compressed. different type of test, employing a non-isothermal regime, was therefore felt to be more appropriate: after some experimentation with different test methods it was decided to measure consolidation *in situ* during an actual processing cycle on a 0·5 m square laminate sample. This was achieved by using a linear variable differential transformer (LVDT) transducer, as in Fig. 6, to measure the through thickness contraction

Table 1 Single point thermal properties for modelling thermal profile during processing

Fabric	Type	Thermal diffusivity, $m^2 s^{-1}$	Thermal conductivity, $W m^{-1} k^{-1}$	Specific heat, $J kg^{-1} k^{-1}$	Density, $kg m^{-3}$
Breather fabric	Airbleed 33N	5×10^{-7}	0·1	800	250
Laminate	Comfil twill weave fabric	$7{\cdot}5 \times 10^{-8}$	0·3	2200	1820

prc0001818 01-04-03 16:38:26 Rev 14.05
The Charlesworth Group, Huddersfield 01484 517077

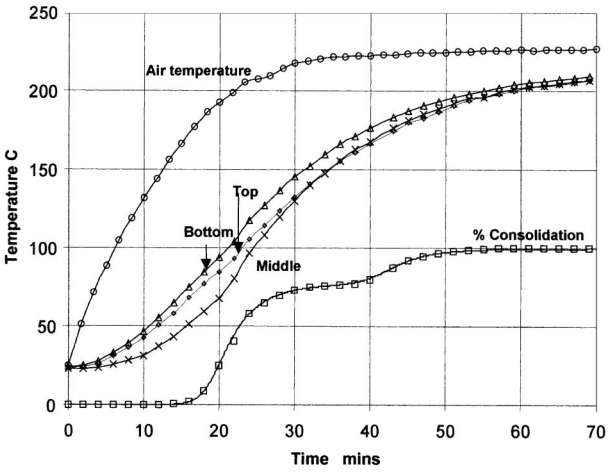

open symbols – experimental data; continuous line – consolidation model, using parameters in Table 2

7 Comfil copolymer processing cycle, showing temperature in oven air and in top, middle and bottom of moulding pack; percentage consolidation also shown

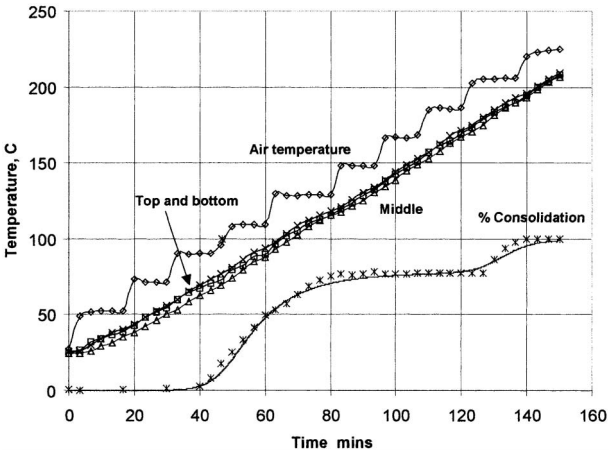

open symbols – experimental data; continuous line – consolidation model, using parameters in Table 2

8 Processing cycle for Comfil copolymer, with slow heating rate achieved by periodically adjusting controller set point – figure shows temperature in oven air and in top, middle and bottom of moulding pack; percentage consolidation also shown

that took place during consolidation. The LVDT itself had to be located outside the processing oven because of its temperature limitations. Since the contraction for a 20 ply laminate was fairly significant – of the order of 10 mm – this quantity was well within the measurement capacity of the LVDT. The method was found to give results that were very reproducible from one processing cycle to the next.

As well as the displacement due to laminate consolidation, there was a small displacement signal due to relative thermal movements between the different components of the rig. The magnitude of this background displacement was determined by recording a full run with bleed fabric and half the normal thickness of laminate, and the LVDT probe touching the surface of the tool instead of the upper surface of the pack. Of course there was no consolidation during this run, as it was not possible to apply a vacuum. The displacement signal from this run provided a small background correction, which was subtracted from the measurements made during consolidation. Finally, the consolidation signal was normalised to give values from 0 to 100% corresponding to the start of the run and the maximum laminate temperature achieved.

Figures 7 and 8 show examples of processing cycles in which both the laminate temperature and consolidation were measured simultaneously. Figure 7 shows a 'typical' cycle, in which it took $\sim$50 min to achieve full consolidation. Figure 8 shows a 'prolonged' cycle, in which the temperature was deliberately raised more slowly, so that the time to full consolidation was increased by a factor of $\sim$3. This was done to test the accuracy and flexibility of the model for different processing conditions. Because the oven was not equipped with a facility for ramping the temperature, the lower rate of heating was achieved by making periodic adjustments to the set temperature, as can be seen from the steplike increases in the air temperature in Fig. 8. Fortunately the steps in the air temperature are damped out by the unsteady state conduction through the laminate.

The processing cycles of different lengths were used to test the ability of both the thermal and consolidation models to describe events occurring over different timescales. It was also found desirable, when fitting rate equations to the consolidation data, to have information on different timescales.

It is interesting to observe that Figs. 7 and 8 both show that consolidation takes place in two distinct stages. The first stage, which is referred to as 'process A', occurs at a temperature near to the T_g of the thermoplastic. This probably involves some solid state stress relaxation and softening of the polymer fibres, accompanied by local deformation, but no bulk flow. This preliminary debulking accounts for a substantial proportion, 78% in the present case, of the total compaction. The second stage, 'process B', occurs over a significantly higher temperature range. This second process is probably a true 'melt' process involving impregnation flow and wetting. Although consolidation is actually driven by the external air pressure on the evacuated laminate pack, both compaction stages can be regarded as being 'thermally' initiated, since it is the achievement of a particular temperature in the laminate pack that really enables the consolidation process to occur.

Two stage consolidation process

The processes, referred to as A and B, are sufficiently far apart in temperature to be modelled separately. In considering the type of model to be applied, some consideration was given of a number of previous models for melt impregnation of fibre beds.[2–15] However, given the surprising result that the greater part of the volumetric consolidation occurs at a relatively low temperature, just above T_g, these models would appear to have limited applicability for process A.

Most of the consolidation models reported in the literature involve Darcy's Law, or adaptations thereof, to describe the flow of melt into the fibre array. This

prc0001818 01-04-03 16:38:26 Rev 14.05
The Charlesworth Group, Huddersfield 01484 517077

well known law states that

$$\frac{dx}{dt} = \frac{Sp}{\eta x} \quad . . . . . (1)$$

where x is the depth of melt penetration, t is the time, S is the permeability, p is the driving pressure and η is the viscosity of the resin.

Most melt impregnation processes have a characteristic flowlength L along which the resin must percolate to achieve full impregnation. It is possible, therefore, to define a degree of impregnation X such that

$$X = \frac{x}{L} \quad . . . . . (2)$$

In the present case it is better to use the more general phrase, 'degree of consolidation', to take account of the fact that process A involves no liquid flow. In addition, the consolidation process is non-isothermal and the viscosity will depend on temperature according to the usual type of Arrhenius relationship, so that

$$\eta = \eta_0 \exp(H/kT) \quad . . . . . (3)$$

where H is the activation energy, k is Boltzmann's constant and T is the absolute temperature.

Incorporating equations (2) and (3) into the expression for Darcy's Law gives a relationship that might be used to describe the temperature dependent evolution of the degree of impregnation

$$\frac{dX}{dt} = \frac{Sp \exp(H/kT)}{\eta_0 X L^2} \quad . . . . . (4)$$

One feature of this model, which is a characteristic of Darcy's Law, is that, for a constant driving pressure, the rate of impregnation declines as the degree of impregnation progresses.

With the present experiments it is tempting to equate the degree of impregnation with the degree of consolidation, as measured by the LVDT experiments. However, questions arise about how to model two processes that are clearly different and separate. For process A, which does not seem to involve any bulk liquidlike flow, Darcy's Law would seem inappropriate. For process B, Darcy's Law was attempted, but did not give a good fit to the results. Since the object of the present study was to provide a tool for process modelling, rather than make a detailed study of the compaction process, it was decided to investigate more widely applicable empirical laws for consolidation.

In the most general case it can be expected that the impregnation rate in a thermally activated process would be given by

$$\frac{dX}{dt} = F(X) \exp(-B/T) \quad . . . . . (5)$$

This can be regarded as a more general version of equation (4). The consolidation rate dX/dt is influenced by two factors: the temperature (through the Arrhenius term); and the level of impregnation. It was possible to produce a master curve giving the form of $F(X)$ *v.* X by choosing an appropriate value of the parameter B (related to the activation energy), since

$$F(X) = \frac{dX}{dt} \exp(B/T) \quad . . . . . (6)$$

Good master curves were obtained for both processes (with different values of B) and it was found that dX/dt decreased as X increased over most of the range. It was necessary, therefore, to consider laws that reflected this.Taking into account models based on Darcy's Law[2–4] for instance, it might be expected that the compaction rate would be inversely proportional to the degree of impregnation, because of the increasing resistance as impregnation proceeds. However, this model did not fit the results; it was found that the compaction rate actually declined much more rapidly than the Darcy Law prediction as each of the two phases reached completion. It was therefore decided to look at an empirical model that would simulate this rapid decline. One such empirical law, often used in the modelling of thermoset cure reactions, is the Kamal equation.[13] This law has not, to the authors' knowledge, been used in the modelling of a purely physical process such as impregnation, but there is no reason why this should not be done. The reduced form of the Kamal equation, shown below, contains four constants.

$$\frac{dX}{dt} = A[\exp(B/T)]X^n(1-X)^m \quad . . . . . (7)$$

An additional constant rate term is often added, since equation (7) presents modelling difficulties because $dX/dt = 0$ when $X = 0$, but this is not needed here. When $n = -1$, $m = 0$, equation (7) corresponds to Darcy's Law.

The term in $(1 - X)$ describes empirically the final decline in impregnation rate. In the present problem, it is not necessary to consider the X dependence of the early part of the impregnation process, so the first term in X can be taken as unity ($n = 0$). The two impregnation phases can be described well by

$$\frac{dX_A}{dt} = A_A[\exp(-B/T)](1-X_A)^{m_A}$$

and

$$\frac{dX_B}{dt} = A_B[\exp(-B/T)](1-X_B)^{m_B} \quad . . . . (8)$$

In addition to the six constants needed to describe the two rate equations, a seventh is needed to represent the respective fractions f contributed to X by each of the two processes, so

$$X = fX_A + (1-f)X_B \quad . . . . . (9)$$

The continuous lines describing the impregnation level in Figs. 6 and 7 were calculated by integrating these equations numerically, using the constants given in Table 2, starting from ($t = 0$, $X = 0$). There is a minor problem, since X_A and X_B appear on the right hand side in equations (8). For data equally spaced

Table 2 Constants used to fit consolidation behaviour of Comfil, based on PET copolymer shown in Figs. 7 and 8

$f = 0{\cdot}78$	A_A and A_B	B_A and B_B	m_A and m_B
Process A	10^{27}	22 500	4
Process B	$3{\cdot}2 \times 10^{31}$	33 000	2·3

prc0001818 01-04-03 16:38:26 Rev 14.05
The Charlesworth Group, Huddersfield 01484 517077

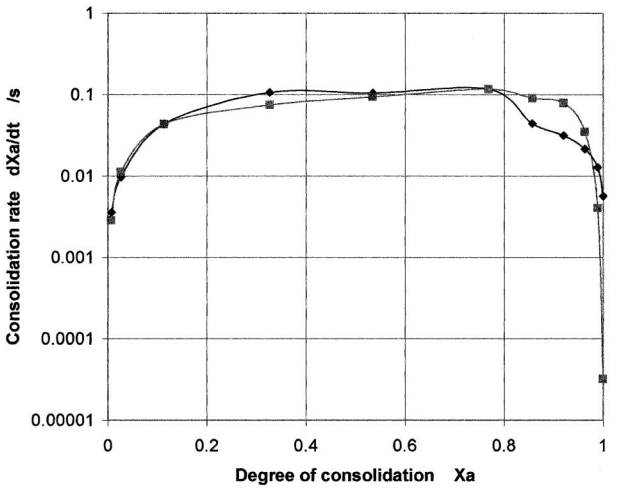

9 Calculated (squares) and measured (diamonds) values of overall consolidation rate in process A, as function of consolidation during process run of Fig. 7

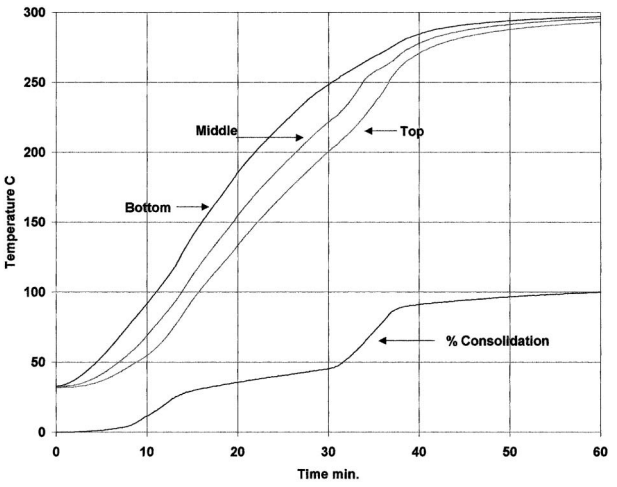

11 Processing cycle for Comfil PET homopolymer, showing temperature in oven air and in top, middle and bottom of moulding pack; percentage consolidation also shown

in time, this can be remedied by trial and error, with an initial quadratic estimate of future values of X, using the finite difference relationship

$$X_{i+1} = 3X_i - 3X_{i-1} + X_{i-2} \quad \ldots\ldots\ldots \quad (10)$$

Figures 9 and 10 show the overall consolidation rates for process A and process B during the run of Fig. 7. The consolidation rate is plotted against degree of consolidation in each case, and it can be seen that there is quite good agreement between the rates measured experimentally and the predictions of the model.

Comparison between behaviour of pet copolymer and homopolymer

Comparing the compaction behaviour of a PET homopolymer based composite with that of one based on the copolymer enables further conclusions to be drawn about the mechanisms of process A and process B. Figure 11 shows a compaction experiment involving the homopolymer (these results will be reported in more detail in a paper currently in preparation). In this case 10 plies of woven fabric were used and the maximum temperature was 295°C.

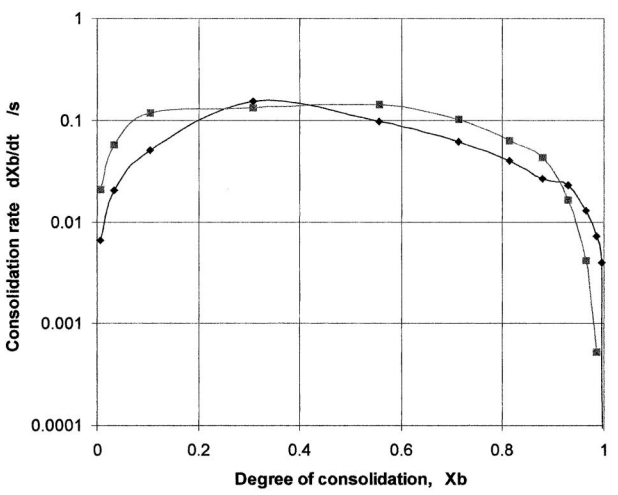

10 Calculated (squares) and measured (diamonds) values of the overall consolidation rate in process B, as function of consolidation during process run of Fig. 7

As with the copolymer, it can be seen that PET homopolymer also shows a two stage consolidation process. In this case, however, process A extends over a broader range of temperature, but accounts for a smaller proportion of the overall consolidation. This would be in keeping with a consolidation mechanism involving compression or compaction of a fibre network. Van Wyck[17] and later Toll,[18] have suggested a relationship of the following form for networks of similar fibres

$$P = kE(X^m - X_0^m) \quad \ldots\ldots\ldots \quad (11)$$

where k is a constant, E is the Young's modulus in bending of the fibres, and X_0 is the degree of consolidation of the system when under no compaction pressure. This model arises from the assumption that the fibres behave as a network of bending beams of circular cross-section, when under compressive load. Often the X_0 term is small enough to allow this relationship to be reduced to

$$P = kEX^m \quad \ldots\ldots\ldots \quad (12)$$

Unfortunately this type of model has yet to be adapted to describe mixtures of fibres, such as glass and PET, but one could well expect a fairly similar type of relationship to apply in this case. The solid state consolidation that occurs around and above T_g may be capable of being modelled mainly in terms of the change in polymer fibre Young's modulus, using a relationship of this type. The fact that the drop in Young's modulus at T_g is much less in the case of the homopolymer, which is semicrystalline, would then account for the lower degree of consolidation in process A. It would also account for the continuing consolidation of the homopolymer over a wider range of temperature, corresponding to the continuing fall in modulus between T_g and T_m.

Finally, the much sharper consolidation of the homopolymer at T_m clearly corresponds to process B, and true melt impregnation. The broader process B in

prc0001818 01-04-03 16:38:26 Rev 14.05
The Charlesworth Group, Huddersfield 01484 517077

the amorphous copolymer is to be expected, because of the gradual decline in viscosity between T_g and temperature at which consolidation actually occurs.

CONCLUSIONS

This project has demonstrated that it is possible to fabricate large structural components from polyester based composites using the relatively simple process of vacuum bag moulding. The significance of this process is that it carries with it a relatively low capital cost penalty, enabling it to be used for short production runs of large components. The applicability of the process extends beyond the lightweight bus sector into general transport, notably rail and small seagoing craft.

The ability to simulate the process by a combination of relatively simple thermal and consolidation models has proved extremely useful in optimising the processing conditions for large parts. *In situ* consolidation measurements were invaluable in process characterisation and monitoring.

The two stage process, in which a significant degree of consolidation takes place in the solid state, has not been reported before for commingled composites. The characterisation technique used here has much to offer in the study of consolidation of composites based on both amorphous and semicrystalline polymers.

ACKNOWLEDGEMENTS

This project formed part of a collaboration between PERA and an industrial consortium, under the Foresight Vehicle LINK and the Structural Materials Programmes. The consortium members were PPG Industries, Trevira Neckelmann a.s, Robert Wright and Son, Advanced Composites Group (ACG) and Hil Technologies.

REFERENCES

1. G. A. ANTONSEN: Proc. Conf. 'Offshore and marine composites', University of Newcastle upon Tyne, 5–6 April, 2000, paper 10.
2. A. G. GIBSON: *Progr. Rubber Plast. Technol.*, 1997, **13**, (2), 125–137.
3. A. G. GIBSON and J.-A. E. MANSON: *Compos. Manuf.*, 1992, **3**, 4.
4. A. MILLER and A. G. GIBSON: *Polym. Polym. Compos.*, 1996, **4**, (7), 459.
5. A. G. GIBSON: in 'Comprehensive composite materials', (ed. A. Kelly and C. Zweben), ch. 2.29, pp 979–997; 2000, London, Elsevier.
6. M. CONNOR, S. TOLL and A. G. GIBSON: *J. Thermoplast. Compos. Mater.*, 1995, **8**, (2), 138–149.
7. A. H. MILLER, N. DODDS, J. M. HALE and A. G. GIBSON: *Composites A*, 1998, **29**, (12), 773–782.
8. T. G. GUTOWSKI, Z. CAI, S. BAUER, D. BOUCHER, J. KINGERY and S. WINEMAN: *J. Compos. Mater.*, 1987, **21**, 650–669.
9. B. P. VAN WEST, R. B. PIPES, M. KEEFE and S. G. ADVANI: *Compos. Manuf.*, 1991, **2**, (1), 10–22.
10. B. P. VAN WEST, R. B. PIPES and S. G. ADVANI: *Polym. Compos.*, 1991, **12**, (6), 417–427.
11. A. C. LONG, C. E. WILKS and C. D. RUDD: *Compos. Sci. Technol*, 2001, **61**, 1591–1603.
12. N. BERNET, M. D. WAKEMAN, P. E. BOURBAN and J.-A. E. MANSON: *Composites A*, 2002, **33**, 495–506.
13. D. J. Y. S. PAGE, P. J. BATES, V. T. BUI and H. W. BONIN: *J. Reinf. Plast. Compos.*, 2000, **19**, 15, 1227–1234.
14. N. SVENSSON, R. SHISHOO and M. GILCHRIST: *J. Thermoplast. Compos. Mater.*, 1998, **11**, 22.
15. M. WYSOCKI: 'Continuum modelling of composites consolidation', PhD Thesis, Chalmers University of Technology, Sweden, 2002.
16. M. R. KAMAL and S. SOROUR: *Polym. Eng. Sci.*, 1973, 13–59.
17. C. M. VAN WYK: *J. Text. Inst.*, 1946, **37**, T285–T292.
18. S. TOLL: *Polym. Eng. Sci.*, 1946, **38**, 1337–1350.

prc0001818 01-04-03 16:38:26 Rev 14.05
The Charlesworth Group, Huddersfield 01484 517077